# Performance evaluation of solar air heater having W-shaped $30^o$ inclined rib as artificial roughness on absorber plate

[1]Shri Krishna Mishra, [2]Himanshu Vasnani, [3]Nagmani Singh
[1,2,3]Assistant Professor, Suresh Gyan Vihar university, Jaipur, India.

**Abstract - The performance of solar air heater is considerably low due to the low value of convective heat transfer coefficient between the flowing air and the absorber plate. An experimental learning has been conceded out for improvement of heat transfer coefficient of a solar air heater which have roughened air duct which is provide with artificial unevenness in the form of W-shaped$30^o$ inclined rib roughened plate as unevenness element. It has been found that on using this absorber plate in solar air heater, the heat transfer coefficient nusselt number values obtained are more then when smooth absorber plate was used. Friction factor values are also reduced fairly. It has also been found that change of pitch from 10 mm to 5 mm also improves the heat transfer coefficient values**

**Keywords: Solar energy; artificial roughness; Nusselt number; Friction factor, Heat transfer coefficient;**

## I. INTRODUCTION

Energy may be generated by fossil fuels. This kind of source of energy is reliable but fossil fuel reservoirs are depleting day by day. So it is a great problem. Renewable energy is the alternate solution to this problem. Of the many alternatives solar energy is considered as the best option. Solar air heaters are the cheapest & most widely used collector devices. The thermal efficiency of solar air heaters is low because of low thermal capacity of air & low heat transfer coefficient between the absorber plate & air flow through duct.

Formation of laminar sub layer on the absorber plate which acts as heat transferring surface leads to low heat transfer coefficient. This laminar sub layer needs to be broken in order to increase heat transfer. In general active & passive techniques are employed to enhance heat transfer between absorber plate & air flow through duct, active techniques requires external forces like electric field. Passive techniques refer to use of special surface geometries such as rough & external surfaces. Artificial roughness is provided below the absorber plate so that turbulence is created in the laminar sub layer.

The solar air heater is considered to be a rectangular channel with one rough surface and three smooth surfaces therefore roughness is provided only on the surface on which solar energy incident. The easiest method of providing artificial roughness on absorber plate is having ribs on the absorber plate. Ribs are of various types like W-shaped ribs, wedge shaped ribs, angled circular ribs, arc shaped etc.

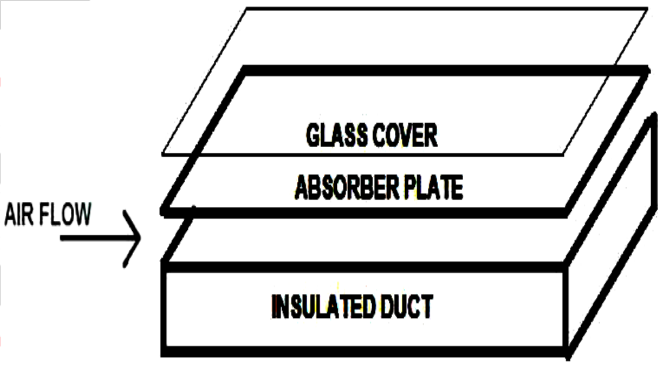


Fig.no.1

The dimensionless geometrical parameters that are used to characterize roughness are:

1. Relative roughness pitch (p/e): It is defined as the ratio of distance between two consecutive ribs and height of the rib.

2. Relative roughness height (e/D): It is the ratio of rib height to equivalent diameter of the air passage.

3. Angle of attack: It is inclination of rib with direction of air flow in duct.

4. Shape of roughness element: The roughness elements can be two-dimensional ribs or three dimensional discrete elements, transverse or inclined ribs or W-shaped continuous or broken ribs with or without gap. The roughness elements can also be arc-shaped wire or dimple or cavity or compound rib-grooved. The common shape of ribs is square but different shapes like circular, semi-circular and chamfered have also been considered to investigate thermo hydraulic performance.

 DOI : 10.18231/2454-9150.2019.0566 

5. Aspect ratio: It is ratio of duct width to duct height. This factor also plays a very crucial role in investigating thermo-hydraulic performance

Many researchers have developed co-relations to investigate the effects of rib shape, pitch to height ratio (p/e) on friction factor and heat transfer. Prasad & Saini (1988) investigated the heat transfer and friction factor in solar air heater using transverse ribs made of copper, glued on the absorber plate. They concluded that increasing p/e ratio (p is the pitch of ribs) beyond about 10 decreases the enhancement in heat transfer. Jaurker et al. (2006) investigated the rib-groove (square rib and triangular groove) roughness arrangement and reported that the heat transfer enhances by 2.75 time and friction factor increased by 3-3.5 times compared to that of the smooth surface. In another study (Layek et al., 2007), the effect of chamfered rib with and without groove was investigated and concluded that the increase in heat transfer coefficient and friction factor for the rib-groove roughness was higher than that of the rib roughness only. Prasad and Mullick (1983) utilized artificial roughness in a solar air heater in the form of small wire to increase the heat transfer coefficients. Prasad and Saini (1988)investigated fully developed turbulent flow in a solar air heater duct with a small diameter profusion wire on the absorber plate Gupta Dhananjayet al. (1997)used continuous ribs of inclination $60^o$ and they optimized thermo hydraulic performance. They found that the optimum operating flow rate shifted to a lower value as the relative roughness height increases. Karwa (2003) has investigated and revealed the effect of transverse, inclined, V-continuous and V discrete patterns on heat transfer and the friction factor in a rectangular duct. The ribs in the V-pattern were tested for both pointing upstream (V-up) and downstream (V-down) to the flow.. Based on the equal pumping power, V-down discrete roughness gave the best heat transfer performance

Hence, the objective of the present work is to conduct experiments to investigate the effect on heat transfer and friction characteristics for artificially roughened W-shaped ribs of 5 mm & 10 mm pitch. In the entire experimentation the values of pitch were taken as 5mm & 10 mm. Other values for different parameters are shown in table.

| **Parameter** | **Values** |
|---|---|
| Reynolds number, Re | 3000–12000 |
| Channel aspect ratio, W/H | 4.0 |
| Test length, L (mm) | 1500 |
| Roughness height, e (mm) | 1 |
| Relative roughness height, e/D | 0.0338 |
| Hydraulic diameter, D (mm) | 160 |
| Roughness pitch (mm) | 5 and 10 mm |
| Insolation, I (W/m2) | 750–880 |

Table 1

## II. EXPERIMENTAL SET UP

A schematic diagram of experimental setup is shown in Fig. 1 The flow system consists of two entry sections, test section and exit section and a centrifugal blower. The three sides of wooden walls the entire length of the duct has a smooth surface while the broad wall is roughened. An unheated entrance duct length of 177 mm is provided. A short entrance length has been chosen because for a roughened duct the thermally fully developed establishes in short length of 2 to 3 hydraulic diameters (D) [1,6]. A 353 mm long exit section is installed to remove any downstream effect on the test section. It may be noted that ASHRAE Standard 93–77 [7] recommends entry and exit length of 2.5 and 5WH, respectively, i.e. 177 and 353 mm, respectively, for the duct. The test section is of 1.5 m length. The top side of the heated test section carries about 1 mm thick G.I. plate with integral rib roughness on the lower side. The top side of the entry and exit lengths of the duct are covered with smooth face 6 mm thick plywood.

The exit end of the duct is connected to a 53 mm diameter pipe provided with an orifice plate to a rectangular to circular transition piece. The air flow rate through the test unit has been regulated with the help of a control valve installed at the inlet of the blower.

Butt welded 0.36 mm copper-constantan thermocouples, calibrated against mercury thermometer of 0.18 centigrade least count, have been used for the temperature measurement. Six thermocouples have been affixed along the axial centre line of the plate in holes drilled 0.5 mm deep into the back of the plate are used to measure variation of the plate temperature.

A 26.5 mm throat diameter orifice plate fitted in a 53 mm diameter pipe with inclined (1:5) U-tube manometer is used to measure the air flow rate. Two absorber plates of G.I. have been prepared having W-shaped $30^o$ inclined ribs with 5 mm & pitch over one side of the plate. Fig. 2 shows the geometry of the absorber plate with the $30^o$inclined ribs. Some difficulties were experienced in getting plates manufactured to the exact dimensions. For the experiment three plates are used. One smooth and two were artificially roughened with roughness pitch of 5mm and 10 mm.

### 2.1 Experimental procedure

The test runs to collect the relevant heat transfer data were conducted under steady state conditions. Five values of flow rate were used for each set of tests. After each change of flow rate, the system was allowed to reach steady state before the data were recorded. The following parameters were measured:

 DOI : 10.18231/2454-9150.2019.0566 

1. Temperature of the heated plate and temperature of air at inlet and outlet of test section of the duct.

2. Pressure difference across orifice meter.

3. Pressure difference across duct.

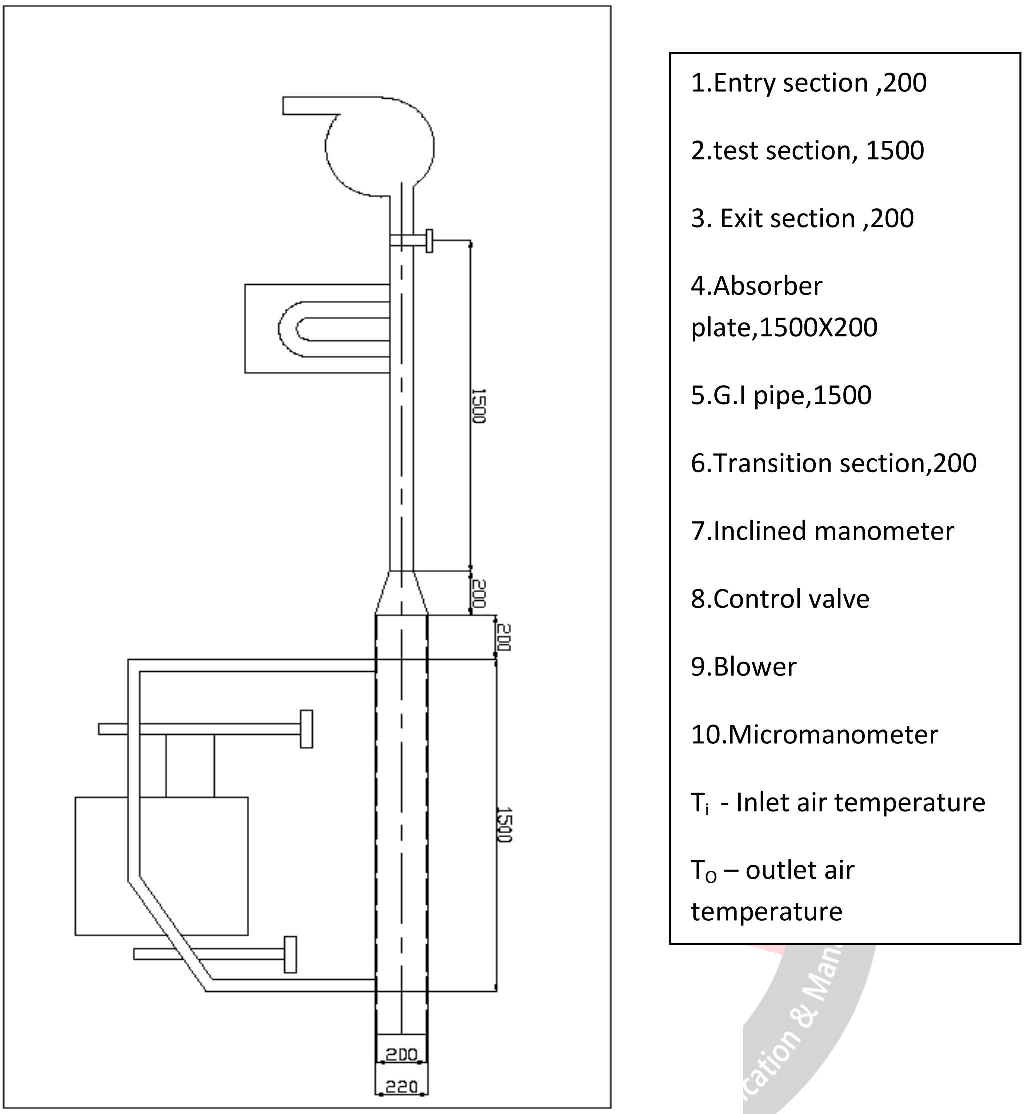


Fig.no.2. **Schematic diagram of the experimental setup**

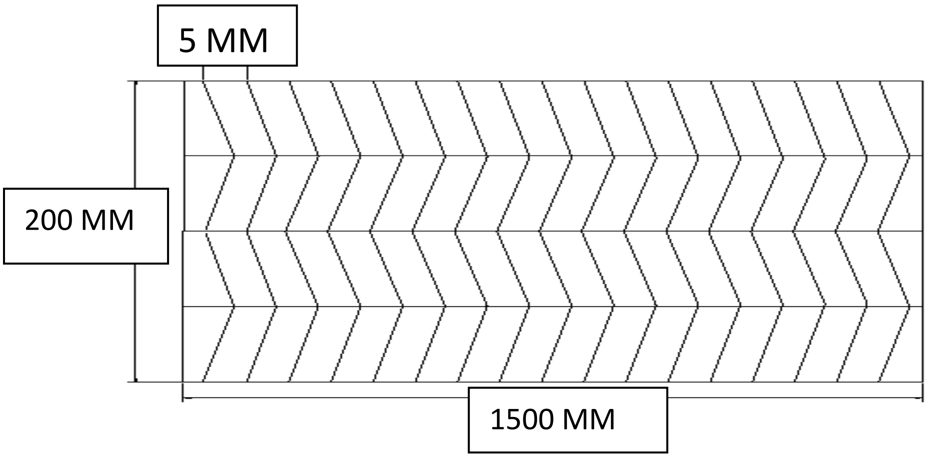


**Fig. no. 3: 5 mm pitch W-shaped 30$^o$ inclined rib roughened plate**


DOI : 10.18231/2454-9150.2019.0566

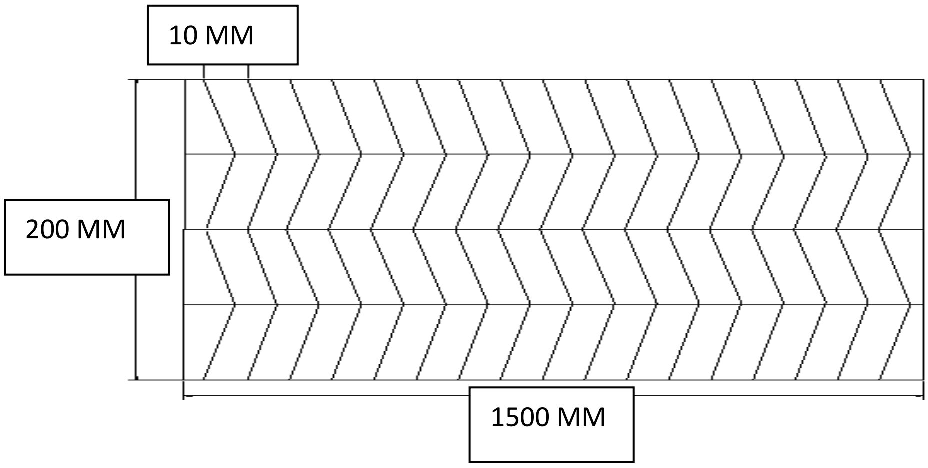


**Fig. no. 4 : 10 mm pitch W-shaped 30° inclined rib roughened plate**

### 2.2 Data reduction

Table 1 shows the experimental parameter and Table 2–5 shows the experimental data for smooth and roughened duct

*3.3.1.2 Mean air and plate temperatures*

The mean air temperature or average flow temperature Tfav is the simple arithmetic mean of the measure values at the inlet and exit of the test section. Thus,

$$T_{fav} = (T_i + T_{oav})/2$$

The mean plate temperature, Tpav is the weighted average of the reading of six points

located on the absorber plate.

*3.3.1.3 Pressure drop calculation*

Pressure drop measurement across the orifice plate was made by using the following relationship

$$\Delta P_o = \Delta h X\ 9.81 X \rho_m X\ 1/5$$

Where

$\Delta P_o$, pressure difference

$\rho_m$ ,density of the fluid

Δh , difference of liquid head in U-tube manometer

*3.3.1.4 Mass flow measurement*

Mass flow rate of air has been determined from pressure drop measurement across theorifice plate by using the following relationship

$$m = C_d X A o[2 X \rho \Delta P_o/(1-\beta^4)]^{0.5}$$

Where

m, mass flow rate, Kg/s

Cd, coefficient of discharge of orifice i.e. 0.62

$A_0$, area of orifice plate, $m^2$

ρ, density of air i.e. 1.1415

β, ratio of dia. ($d_0/D_p$) i.e. 26.5/53 = 0.5.

*3.3.1.5. Velocity measurement*

$$V = m/\rho WH$$

where

m, mass flow rate, Kg/s

ρ, density of air i.e. 1.1415 Kg/m3

H, height of the duct, m (0.025)

W, width of duct, m (0.2).

*3.3.1.6 Reynolds number*

 DOI : 10.18231/2454-9150.2019.0566 

The Reynolds number for flow of air in the duct is calculated from

$$\mathbf{Re = V \times D/\upsilon}$$

$\upsilon = 16.7 \times 10^{-6}\ m^2/s$

Hydraulic diameter $D$ = 4 WH/2(W+H)

*3.3.1.7 Heat transfer coefficient*

Heat transfer rate, $Q_a$, to the air is given by

$$Q_a = mC_p\,(T_o - T_i)$$

The heat transfer coefficient for the heated test section has been calculated from

$$h = Q_a/A_p \times (Tpav - T_{fav})$$

$A_p$ is the heat transfer area assumed to be the corresponding smooth plate area.

3.3.1.8. Nusselt number

The heat transfer coefficient has been used to determine the Nusselt number and Stanton number defined as:

$$\mathbf{Nu = hD/k}$$

where k is the thermal conductivity of the air at the mean air temperature and D is the Hydraulic diameter based on entire wetted parameter.

3.3.1.9 .Thermo hydraulic Performance

$$THP = \frac{Nu_{rough}/Nu_{smooth}}{\left(f_{rough}/f_{smooth}\right)}$$

| S. no | Reynolds number (Re) | Inlet temp. Ti ($^0$C) | Avg. outlet temp. Toav ($^0$C) | Avg. fluid temp. Tfav($^0$C) | Avg. plate temp. Tpav($^0$C) | Toav–Ti ($^0$C) | Tpav–Tfav ($^0$C) | Conv. Heat transfer co. h (W/m2 $^o$C) | Nusselt number (Nu) | Friction Factor(f) |
|---|---|---|---|---|---|---|---|---|---|---|
| 1 | 3000 | 37 | 64 | 50.5 | 128 | 27 | 77.5 | 7.563 | 10.042 | 0.0115 |
| 2 | 5000 | 38 | 61 | 49 | 109 | 23 | 59.5 | 9.487 | 16.324 | 0.0108 |
| 3 | 8000 | 38 | 59 | 48.5 | 90 | 21 | 41.5 | 11.334 | 17.556 | 0.0105 |
| 4 | 10000 | 39 | 58 | 48.5 | 82 | 19 | 33.5 | 13.253 | 18.837 | 0.0098 |
| 5 | 12000 | 40 | 57 | 48.5 | 78 | 17 | 29.5 | 15.495 | 19.07 | 0.0091 |

**Table 2 Experimental data for smooth plate**

| S. no | Reynolds number (Re) | Inlet temp. Ti ($^0$C) | Avg. outlet temp. Toav ($^0$C) | Avg. fluid temp. Tfav($^0$C) | Avg. plate temp. Tpav($^0$C) | Toav–Ti ($^0$C) | Tpav–Tfav ($^0$C) | Conv. Heat transfer co. h (W/m2 $^o$C) | Nusselt number (Nu) | Friction Factor(f) | T.H.P. |
|---|---|---|---|---|---|---|---|---|---|---|---|
| 1 | 3000 | 39 | 61.5 | 50.25 | 130 | 22.5 | 68.5 | 6.84922 | 10.98653 | 0.023 | 1.2746 |
| 2 | 5000 | 40 | 59 | 49.5 | 108 | 19 | 49 | 11.48406 | 17.53649 | 0.0224 | 1.4627 |
| 3 | 8000 | 41 | 55 | 48 | 97 | 14 | 42 | 11.90093 | 29.96768 | 0.0204 | 1.6278 |
| 4 | 10000 | 41 | 54 | 47.5 | 84 | 13 | 30 | 23.98907 | 37.09654 | 0.0196 | 1.8669 |
| 5 | 12000 | 41.5 | 52 | 46.75 | 74 | 10.5 | 22 | 26.48162 | 40.48475 | 0.0091 | 1.8067 |


DOI : 10.18231/2454-9150.2019.0566

**Table 3 Experimental data for W-shaped roughened 10 MM pitch plate**

| S. no | Reynolds number (Re) | Inlet temp. Ti ($^0$C) | Avg. outlet temp. Toav ($^0$C) | Avg. fluid temp. Tfav($^0$C) | Avg. plate temp. Tpav($^0$C) | Toav–Ti ($^0$C) | Tpav–Tfav ($^0$C) | Conv. Heat transfer co. h (W/m2 °C) | Nusselt number (Nu) | Friction Factor(f) | T.H.P. |
|---|---|---|---|---|---|---|---|---|---|---|---|
| 1 | 3000 | 38 | 63 | 55.5 | 134 | 25 | 83.5 | 6.84922 | 10.98653 | 0.023 | 0.94283 |
| 2 | 5000 | 39 | 60.5 | 49.75 | 111 | 21.5 | 61.75 | 11.48406 | 17.53649 | 0.0224 | 1.57643 |
| 3 | 8000 | 40 | 57 | 48.5 | 95 | 17 | 46.5 | 16.90093 | 27.96768 | 0.0204 | 1.36464 |
| 4 | 10000 | 41.5 | 55 | 48.25 | 79 | 13.5 | 30.75 | 21.98907 | 34.09654 | 0.0196 | 1.9865 |
| 5 | 12000 | 41.5 | 54 | 47.75 | 77 | 12.5 | 29.25 | 25.48162 | 38.48475 | 0.0191 | 1.4645 |

**Table 4 Experimental data for W-shaped roughened 5 MM pitch plate**

## III. RESULTS & DISCUSSION

In the present investigation the effect of various flow and roughness parameters on heat transfer characteristics for flow of air in rectangular ducts of 5 MM & 10 MM pitch W-shaped absorber plate are discussed below. Results have also been compared with those of smooth ducts under similar flow and geometrical conditions to see the enhancement in heat transfer coefficient.

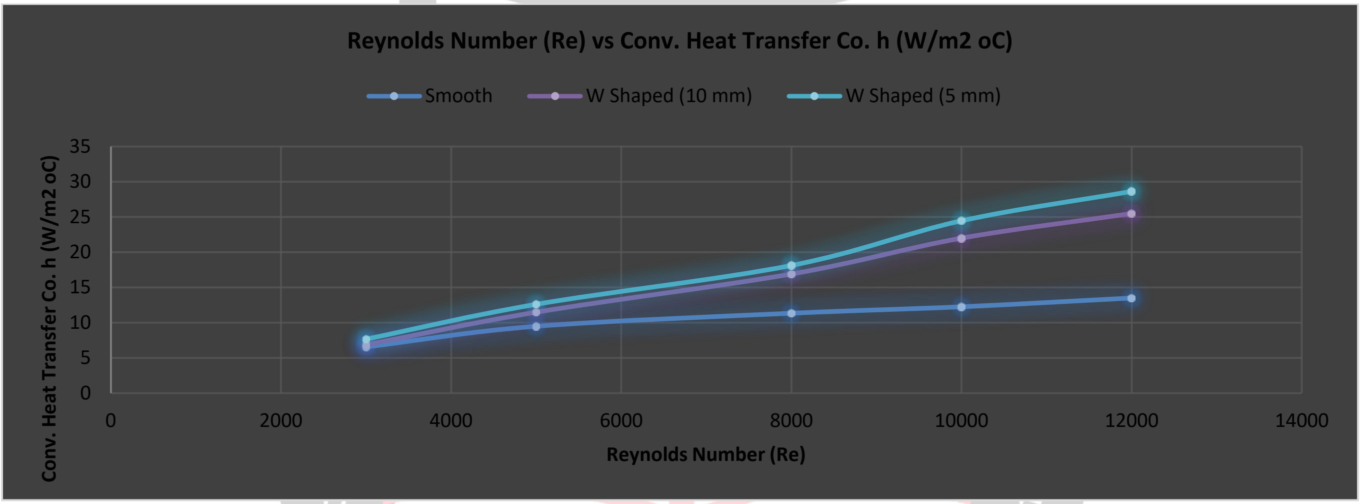


**Fig.5 Comparison of heat transfer coefficient values for different roughness plates**

It can be seen from the Fig.5, the values of heat transfer coefficient increases with increases in Reynolds number. The increase of h values with increase in Re for 10 mm pitch W-shaped roughened plate is higher than that of smooth plate. This increase is even higher for 5mm pitch W-shaped roughened plate Another observation drawn from the comparison of h vs Re graph of different plates is that for low Reynolds number, change in heat transfer coefficient is negligible with respect to roughness pitch, because when Reynolds number is low (<5000) the thermal boundary layer remains unbreakable, which offers resistance to heat flow and hence low heat transfer coefficient may result.

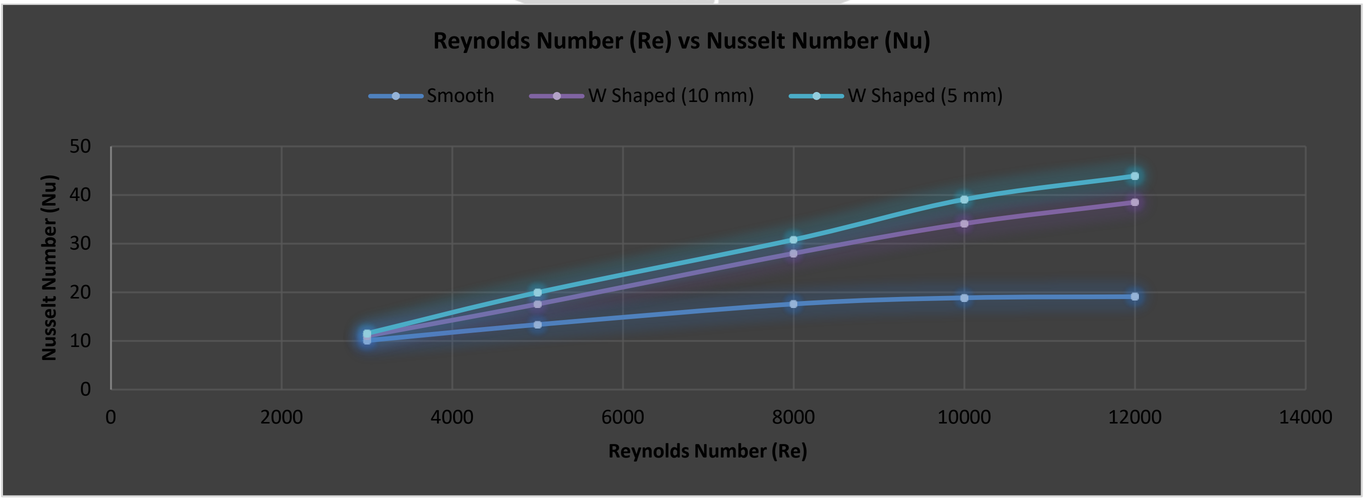


**Fig.6 Comparison of Nusselt number values for different roughness plate**


DOI : 10.18231/2454-9150.2019.0566

It is clear from the Fig.6, that the values of Nusselt number increases with increase in Reynolds number .But this increase is not the same for all plates of different roughness geometries & pitch. The increase of Nusselt number with respect to Reynolds number is not as high for smooth plate as for all other $30^0$ inclined rib roughened plates. The increase of Nu values with increase in Re for 10 mm pitch W-shaped roughened plate is higher than that of smooth plate. This increase is even higher for 5mm pitch W-shaped roughened plate

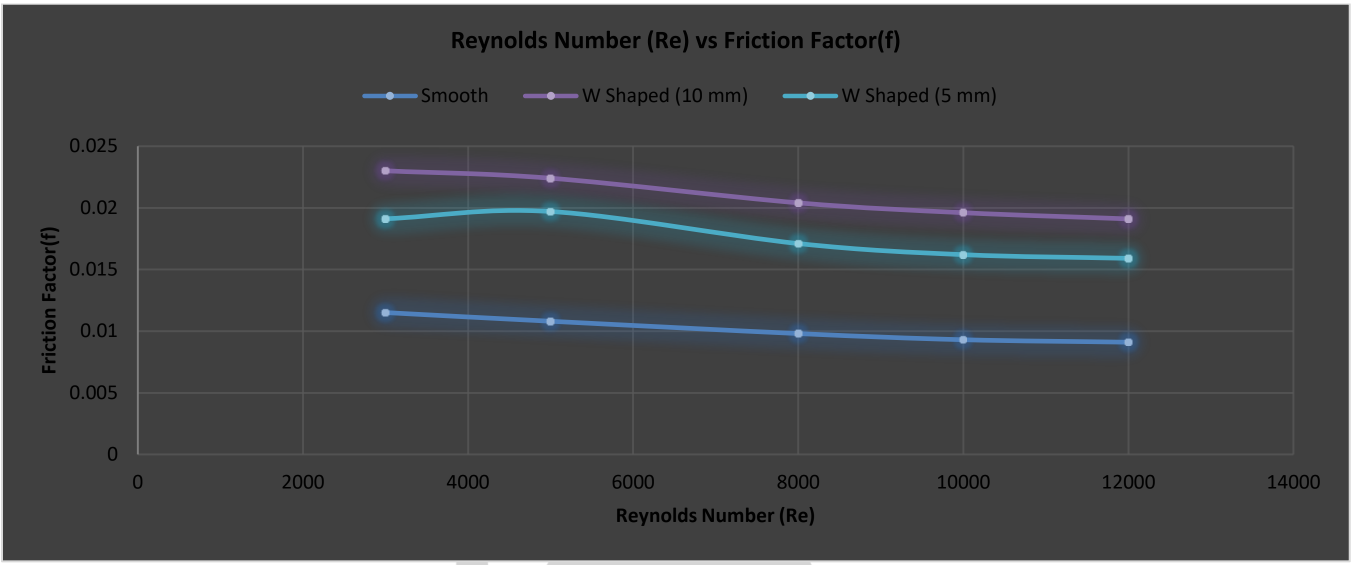


**Fig.7 Comparison of friction factor values for different roughness plates**

Fig.7 shows the data regarding variation of friction factor with Reynolds number for different $30^o$ rib roughened plate of 5mm & 10 mm pitch and smooth plate. As we know that by increasing the Reynolds number the viscous sub layer near the surface of roughened absorbing plate get suppressed which proportionally decrease the value of friction factor with increase in Reynolds number

## IV. Conclusion

The present work was undertaken of with the objective of extensive investigation into the $30^o$ inclined W-shaped ribs as artificial roughness on the underside of one broad wall of solar air heater. Results have to be compare with those of even and smooth duct under like flow conditions to establish enhancement in heat transfer coefficient & friction factor.

The following conclusions have been drawn from this investigation:

1. Convective heat transfer coefficient increases with increase in Reynolds number for W-shaped& W-shaped $30^o$ inclined rib roughened plates of 5 mm & 10 mm pitch.

2. In the entire range of Reynolds number it is found that Nusselt number increases with increase in Reynolds number.

3. The value of Nusselt number increases with decrease in the value of pitch.

But the value of Nusselt number for 5mm W-shaped $30^o$ inclined rib roughened is slightly greater than 10mm W-shaped rib roughened plate

4. Roughened absorber plate increases the heat transfer coefficient 1.25 -1.4 times as compared to smooth rectangular duct under similar operating conditions at higher Reynolds number.

5. For low Reynolds number, change in heat transfer coefficient is negligible with respect to roughness pitch.

6. The value of friction factor decreases with increase of Reynolds number for different roughness geometries.

## References

[1] Karwa, R. Solanki, S.C. and Saini, J.S., (1999) Heat transfer coefficient and friction factor correlations forthe transitional flow -roughened rectangular duct, *Int. Journal of Heat Mass Transfer*, 42, pp. regimes in rib 1597 -1615.

[2] Dhananjay, Gupta, Solanki, S.C Saini, J.S.1997. Thermo hydraulic performance of solar air hearers with roughened absorber plates. Solar Energy 61, 33–42.

[3] Prasad, B.N. and Saini, J.S., (1988). Effect of artificial roughness on heat transfer and friction factor in solar air heater, *Solar Energy*, 41, pp. 555 – 560

[4] Prasad, K., Mullick, S., 1983. Heat transfer characteristics of a solar air heater used for drying purposes. Appl. Energy 13, 83–98.

[5] Layek, A. Saini, J.S. and Solanki, S.C., (2007). Heat transfer and friction characteristics for artificiallyroughened duct with compound turbulators, *International Journal of Heat and Mass Transfer*, 50, pp. 4845 – 4854.

[6] Jaurker, A.R. Saini, J.S. and Gandhi, B.K., (2006). Heat transfer and friction characteristics of rectangular solar air

 DOI : 10.18231/2454-9150.2019.0566 

ISSN : 2454-9150 Special Issue - TMRI - 2019

heater duct using rib-grooved artificial roughness, *Solar Energy*, 80, pp. 895 – 907.

[7] G. Alvarez, J. Arce, L. Lira, M.R. Heras(2004) Thermal performance of an air solar collector with an absorber plate made of recyclable aluminum cans.

[8] A. Hachemi (1998) Experimental study of thermal performance of offset rectangular plate fin absorber plates.

[9] A.P. Omojaro, L.B.Y. Aldabbagh (2010) Experimental performance of single and double pass solar air heater with fins and steel wire mesh as absorber

## NOMENCLATURE

| | | | |
|---|---|---|---|
| A | area of absorber plate, m2 | P | wire pitch |
| A | duct flow cross-section area ZWH, m2 | Qa | useful heat gain, W |
| $A_o$ | throat area of orifice meter, m2 | Re | Reynolds number |
| $A_p$ | plate heat transfer area, m2 | $T_a$ , $t_a$ | atmospheric temperature, 8C |
| $C_d$ | coefficient of discharge | $T_i$, $t_i$ | air inlet temperature, 8C |
| $C_p$ | specific heat, J/kg k | $T_{fav}$ | average flow temperature of air, 8C |
| D | channel hydraulic diameter, m | $T_{oav}$ | average outlet temperature of air, 8C |
| $D_p$ | inside dia of pipe, m | V | velocity of fluid in pipe, m/s |
| $D_o$ | diameter of orifice of the orifice plate, m | W | duct width, m |
| H | depth of the duct, m | W/H | channel aspect ratio |
| h | convective heat transfer coefficient, W/m2 k | Symbols | |
| I | solar insolation, W/m2 | b | diameter ratio |
| K | thermal conductivity of air, W/m k | $\eta_{th}$ | thermal efficiency |
| L | test section length, m | n | kinematic viscosity, m2/s |
| M | mass flow rate, kg/s | | |
| Nu | Nusselt number | | |

 DOI : 10.18231/2454-9150.2019.0566 